ORIGINAL ARTICLE

Hydro-chemical analysis and ionic flux of meltwater runoff from Khangri Glacier, West Kameng, Arunachal Himalaya, India

Harish Bisht[1] · Prakash Chandra Arya[2] · Kireet Kumar[1]

Abstract

The detailed hydro-chemical study of meltwater draining from Khangri glacier Arunachal Pradesh has been carried out to evaluate the major ion chemistry and weathering processes in the drainage basin. The investigative results shows that the meltwater is almost neutral to slightly acidic in nature with $Mg–HCO_3$-dominated hydro-chemical facies. In glacial meltwater, Ca^{+2} is the most dominated cation followed by Mg^{+2}, Na^+, and K^+, while HCO_3^- is the most dominant anion followed by SO_4^{2-}, NO_3^-, and Cl^-. The dominant cations such as Ca^{+2} and Mg^{+2} show a good relation with the minerals abundance of the rocks. Calcite ($CaCO_3$) and biotite $[K(Mg,Fe)_3AlSi_3O_{10}(F,OH)_2]$ are the most abundant minerals in the deformed carbonate-rich metasedimentary rocks near to the snout with some K feldspar ($KAlSi_3O_8$) and quartz (SiO_2). This suggests Ca^{+2} have definitely entered into the water due to the dissolution of calcite and Ca feldspar ($CaAl_2Si_2O_8$), while one of the source of Mg^{+2} is biotite. Na feldspar ($NaAlSi_3O_8$) has contributed towards the availability of sodium ion, while potassium ion is derived from the chemical weathering of K feldspar and biotite. The chemical weathering is the foremost mechanism controlling the hydro-chemistry of the Khangri glacier because of the least anthropogenic interferences. The mineralogy of surrounding rocks is studied to understand better, the rock–water interaction processes, and their contribution towards ionic concentration of meltwater. The meltwater discharge and individual ion flux of the catchment area have also been calculated, to determine the ionic denudation rate for the ablation season. The high elemental ratio of $(Ca+Mg)/(Na+K)$ $(7.91\pm0.39$ mg/l) and low elemental ratio of $(Na+K)$/total cations (0.11 ± 0.004) indicate that the chemical composition of meltwater is mainly controlled by carbonate weathering and moderately by silicate weathering. The scatter plot result between $(Ca+Mg)$ and total cations confirms that carbonate weathering is a major source of dissolved ions in Khangri glacier meltwater. In addition, the statistical analysis was also used to determine the correlation between physical parameters of glacier meltwater which controlled the solute dynamics.

Keywords Carbonate weathering · Hydro-chemical facies · Khangri glacier · Meltwater · Mineralogy · Solute dynamics

Introduction

The Himalayan region comprises of a total 9575 glaciers which covers an area of around 40,000 km^2 (Raina and Srivastava 2008). In the Himalayas, about 14,000 cubic km of snow and ice is locked in high altitude regions (Valdiya 1998), which contributes towards considerable runoff of most of the Himalayan rivers (Singh et al. 2008). The anthropogenic interference is generally less in glacial environments, which makes it ideal for studying control of natural processes on the quality of stream water (Brown and Fuge 1998a). The chemical activity is more intense in glaciated regions than in tropics (Souchez and Lemmens 1987). In glaciated regions, the high rate of chemical weathering is mainly due to long residence time of meltwater with the

✉ Harish Bisht
  harishbisht890@gmail.com

  Prakash Chandra Arya
  aryapraky@gmail.com

  Kireet Kumar
  kireet@gbpihed.nic.in

[1] G.B. Pant National Institute of Himalayan Environment and Sustainable Development, Kosi-Katarmal, Almora, Uttarakhand 263643, India

[2] Indian Institute of Science, Bangalore, Karnataka 560012, India

bedrock (Singh et al. 2012). Hydro-geochemical investigation of glacier meltwater is helpful in identifying the concentration and nature of solute present in the basal lithology and atmosphere (Ramanathan 2011). The hydro-chemical study of Himalayan glacier meltwater is crucial with the advancement of geochemical studies as well as increasing demands of fresh water in downstream areas. It is also important to assess the contribution of weathering reactions and climatic changes which can influence the chemical properties of meltwater. The chemical composition of meltwater varies for different glaciers, and much of this variation might be attributed to different lithology (Collins 1979a; Ramanathan 2011). Some studies (Godsey et al. 2009; Clow and Mast 2010) also suggest that weathering of primary minerals provides solutes, which mainly control the chemical composition of stream. However, sometimes, there is a considerable variation in hydro-chemical properties between the rivers draining in similar lithologies (Oliva et al. 2003), which is probably due to atmospheric input. The atmospheric CO_2 reacts with the water and forms a weak carbonic acid which is responsible for chemical weathering of bedrock (Singh et al. 2012). Chemical weathering is an integrated process resulting from the interaction between rock, water, and atmosphere. The effectiveness of these constituents mainly depends on the size of particle, composition of rock, favorable temperature, and humidity condition.

The exact hydro-chemical characterization of certain environment is difficult due to the addition of water through several sources in glacial catchment (Collins 1979a). In the present study, a total of 22 meltwater samples were collected from the location (Fig. 1), near to the snout of the Kangari glacier in clear weather days to avoid the effect of atmospheric input (rainfall and snowfall). Some studies have been conducted in the Tawang and West Kameng region including snow melt runoff modeling (Senzeba et al. 2015), temporal variation in wet and dry snow cover (Bhadra et al. 2016), study of hot springs (Bora et al. 2006), geochemistry of granitoids (Srivastava 2013), and Geology of Tawang (Bhattacharjee and Nandy 2007). However, to the best of our knowledge, there have been no attempts made so far to study the glacial meltwater hydro-chemistry of eastern Himalayas (Arunachal Pradesh), most probably because it is one of the most inaccessible places on Earth, located at ~5000 m above mean sea level (MSL). Reaching to Khangri glacier near to Gori-Chin Mountain took almost 4 days of walking in the glacial valleys, which covers a total distance of 70 km, and the path is full of landslides, debris and large boulder at many places, along with low oxygen level which makes it difficult to walk. In this region, a healthy person can cover a maximum of 17–20 Km in 1 day. At night, the temperature usually falls below freezing point. These are some of the reasons which have created a large gap in the literature of the glacial dynamics, meltwater discharge, hydrochemistry, and weathering process. At present, very little is known about the processes operating in the higher altitudes of N–E Himalayas. This specific study has been carried out to determine the major ion chemistry of meltwater draining from the Khangri glacier and its relation with the mineral

Fig. 1 Location map of the study area
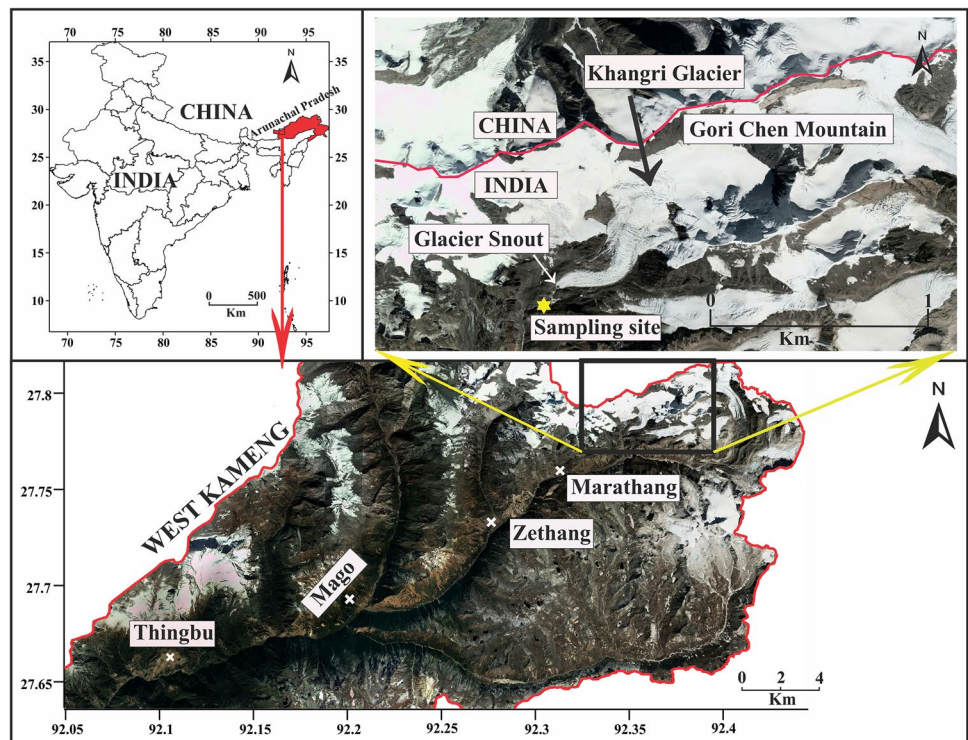
composition of surrounding rocks. In addition, this study was designed to investigate the weathering processes which affect the chemical composition of glacier meltwater.

Study area

Arunachal Pradesh is the northeastern most state of India lying between the latitude 26°40′ and 29°25′N to longitude 91°35′ and 97°25′E, known as land of dawn-lit mountains (Kumar 2013). The Khangri glacier has been selected for the present study, which is situated in the West Kameng district of Arunachal Pradesh which lies between the higher Himalaya and Tethys Himalaya (Fig. 1). The monsoon period is from May to September month with an average annual precipitation of 1139 mm (Senzeba et al. 2015). Geographically, the glacier is located between (27°46×59.3″ and 27°48×5.6″N–92°21×18.1″ and 92°22×2.4″E) at

Gori-Chen Mountain bordering the China. It is NE–SW flowing valley-type glacier, flowing towards SW (210° N), situated at an altitude of around 5000–5500 m above MSL. The accumulation zone of this glacier is at Gori-Chen Mountain located at an altitude of ~6000 m above MSL. The snout of this glacier (27°46×59.3″ N and 92°21×18.1″ E) is located at an altitude of 4909±2 m above MSL (measured through GPS Etrex 30). The front of this snout is fan shaped, convex downwards which covers a large area of the glacial valley. The upper part of this glacier is devoid of debris cover, while the lower part near snout partially covered with debris. Glacial striations are common on the rocks exposed near to the snout (Fig. 2a), which is an evidence of the past glaciers movements and its vigorous dynamics. The glacier erosion and deposition is responsible for formation of a wide U-shaped valley, a variety of other glacier landform (Hanging Valley, Glacial Striations, Kettle Lakes, and Lateral and Terminal Moraines) are extensively present

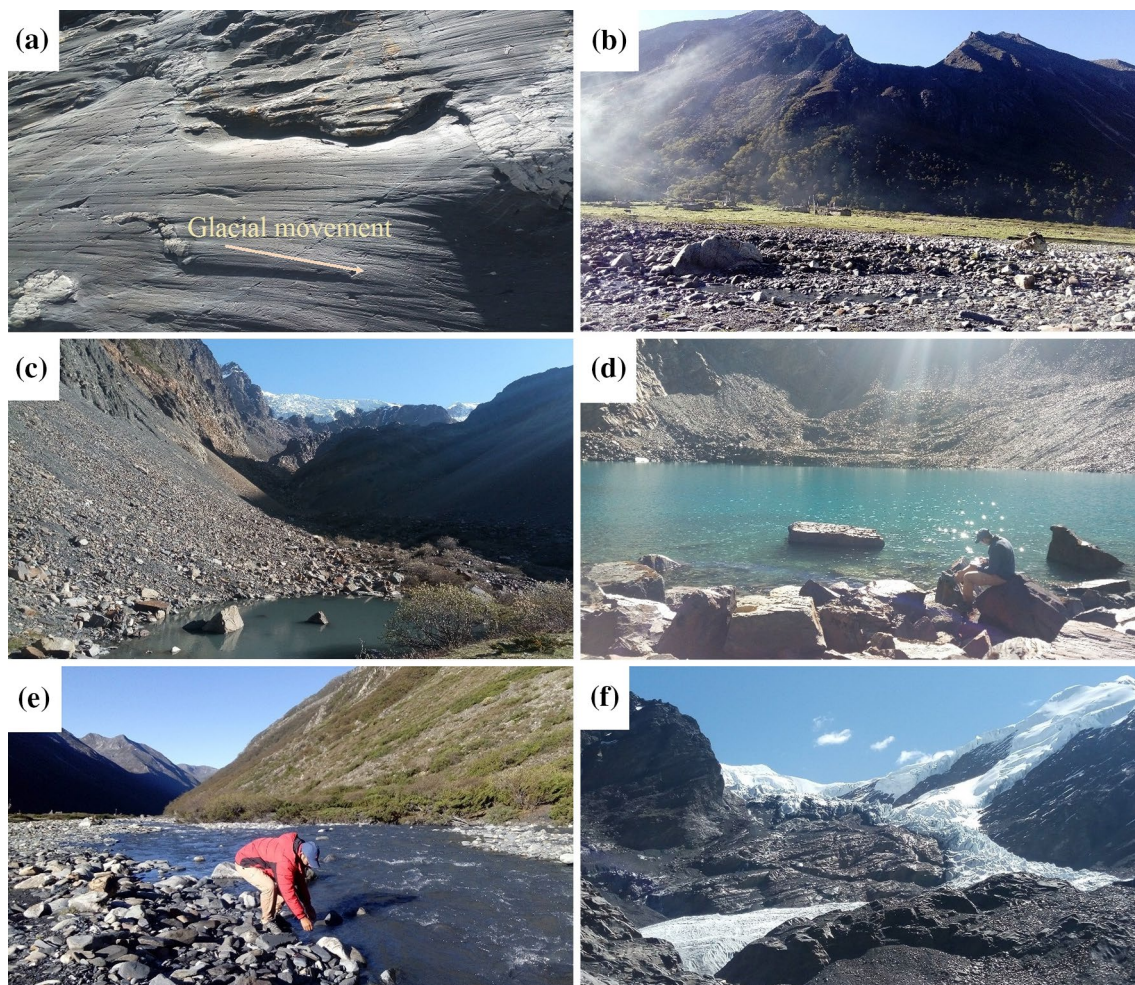**Fig. 2** **a** Glacial striations on surface of the bedrock near the glacier snout. **b** Flat land completely made up of silt and clay with clearly visible hanging valley. **c** Small kettle Lake 2–3 km downstream of the glacial snout. **d** Large kettle Lake near to the snout. **e** Glacial meltwater sample collection site. **f** Slightly metamorphosed sedimentary shale and slate near the glacial snout

and well preserved in the study area. Throughout the valley, extensive evidences of the past glacial movements were observed by well-developed lateral moraines and valley fills. The large flat ground is present on the right bank of Khangri river known as Zethang and Marathang, completely made up of silt and clay, which is a good evidence of an old-dried glacier lakes (Fig. 2b). These two flat grounds represent a lacustrine plain presently an alpine meadow which supports the diversified alpine flora. On the top of these flatlands, glacial hanging valley can be easily identified which were formed as a result of extinction of a tributary glacier which was once connected to the main glacier (Fig. 2b). The several glacial kettle lakes were present near to the snout, ranging in size from 500 m long and 260 m wide to 30 m long and 20 m wide (Fig. 2c, d). The present landform in and adjoining area of glacier is an integrated results of glacier dynamics and tectonic movements.

General geology

The western Arunachal encompasses rockstypes from Siwalik to the crystallines of higher Himalayas (Bhattacharjee and Nandy 2017). Bakliwal and Das (1971) carried a detailed fieldwork along Bhalukpong-Sela in 1971, and classified the rocks into Sela Group, Bondila Group, Bichom Group, Tenga Formation, Gondwana, and Siwalik. Arunachal Himalayas have suffered four episodes of granite activity which comprises of biotite bearing granite (Salari), tourmaline-bearing granite (Higher Himalayan leucogranite) and two (Bomdila and Zimithang granite) mica-bearing porphyritic granite gneiss (Bhattacharjee and Nandy 2017). Later, few researchers carried out geological mapping in the Tawang and West Kameng districts, viz, Jain and Basu (1978), Tripathi et al. (1979) and Singh (1998). They mapped a metasedimentary sequence comprising of schist and quartzite tectonically underlying the Sela and Bomdila Group of rocks and named it as the Luma Formation. The western part shows a thrust bound lithounits comprising the migmatitic gneiss of the Sela Group intruded by Tertiary leucogranite, the Zimithang granite, granite gneiss, metasediments of Luma and Dirang Formations, quartzite and dolomite of the Bomdila Group, siltstone of Siwalik Group, and oceanic facies of Gondwana (Bhattacharjee and Nandy 2017). A general tectono-stratigraphic succession of the western Arunachal Himalaya is given in Table 1. The study area mainly comprises the granite gneiss and tourmaline-bearing granite with large amount of metasedimentary rocks near the snout of the glacier. Some amount of schist and quartzite are also present in the downstream nearby area of Thimbu. The Zimithang granite occurs as a large batholiths and tourmaline-bearing leucogranite intruded into the migmatite of Sela Group. The metamorphic grade increases from the base of Dirang formation to the top of Sela Group.

The Selas are thrust over the metasedimentary rocks of Dirang formation and the thrust is termed Main Central Thrust (MCT) (Bhattacharjee and Nandy 2017). In addition, the Bomdila Gneiss forms a part of lesser Himalayan sequence are thrusted over the Gondwana along the Main Boundary Fault (MBT) (Bhattacharjee and Nandy 2017). In the present study, five different rock types were encountered while taking a traverse from SSW to NNE along the bank of river, in a direction opposite to the flow of the river, from (Jang) to the snout of Khangri glacier (Fig. 3). The rock types encountered successively are (1) schist/quartzite; (2) leucogranite; (3) biotite containing pink granite; (4) micaceous sandstone; and (5) carbonate-rich shale/slate. The schist, quartzite, and sandstone belong to the Thingbu Formation of the Upper Proterozoic time (Table 1), which are low-grade micaceous quartzite and sandstones and are well exposed near to the Thingbu village (Fig. 3). These micaceous sandstones and quartzites are intruded by biotite granite and leucogranites, which belongs to Dailing Formation of Bomdila Group of rocks (Table 1) and are well exposed in the north of Thingbu and Mago village (Fig. 3). Towards the north of Thingbu sandstone, calcareous rocks are exposed until the snout of glacier which are very similar to those of Niumi unit, Dedza Formation of Bomdila group of rocks (Middle Proterozoic) (Table 1). The metasedimentary rocks in the study area are of Proterozoic times which are intruded by granitic melt. Among the granitic bodies, biotite containing pink granite encloses the feldspar grain providing a shape of an augen, these characteristics are very much similar to Bomdila granite explained by Bhattacharjee and Nandy (2017). The leucogranite is rich in muscovite with small (up to 0.5 cm) needles of tourmaline, the muscovite of the granite glitters like mirror when sunlight falls at some angle to the granite. The leucogranite is equigranular in texture, while the Bomdila granite is porphyritic with large (up to 2.5 cm) feldspar grains. The micaceous sandstone is a orange–brown colored sandstone with thin laminations due to the presence of micaceous mineral it has developed a mild schistosity. The dark-colored carbonate-rich shale/slate exposed near the snout containing two sets of striations, with white elongated sinuous calcite veins.

Materials and methods

Sample collection

To determine the hydro-chemistry of meltwater, sampling site was selected near the snout of glacier (Fig. 1), where no other tributary glacier meltwater meets with the main stream. The total 22 meltwater samples were collected, and all water samples were collected near base camp (27°46×19.1″N and 92°21×5.1″E) located at 1 km downstream of the present

Table 1 General tectono-stratigraphic succession of the western Arunachal Himalaya after Bhusan et al. (1991) and Kesari (2010)

| Age	Group	Formation	Member/ Uint	Lithology/Properties
Quaternary		Hapoli		Sand, clay and peat
--Frontal Thrust--				
Mio Pliocene	Siwalik	Kemin		Boulder conglomerate, pebble sandstone
Mio Pliocene		Subansiri		Salt and pebble lithic arenite
Miocene		Dafla		Micaceous sandstone with calcareous concretions
---Main Boundary Thrust (MBT)---				
Early to Middle Eocene	Yinkiong	Dalbuing		Limestone with shale intercalation
Late Palaeocene to Early Eocene		Geku		Purple, pale green and black shales, sandstones, quartzite
---Unconformity---				
Upper Permian	Gondwana	Yamne		Pale brown ferruginous shale
Permo-Carboniferous		Bhareli	Upper	Feldspathic sandstone, black carbonaceous shale
			Lower	Arkosic red sandstone and siltstone, black carbonaceous shale
Permo-Carboniferous		Bichom	Upper (Sesa)	Grey to black tuffaceous shale with impersistant bands of quartzite
			Middle (Bomte)	Grey to black shale with calcareous and phosphatic chert nodules
			Lower (Rilu)	Diamictite with subordinate sandstone, shale and grits
Lower Palaeozoic		Miri		Purple to pinkish, white to grayish feldspathic quartzite, purple micaceous shale, diamictite conglomerate
Upper Proterozoic		Thingbu		Low grade carbonaceous mica schist and micaceous quartzite
---Unconformity---				
Middle Proterozoic		Dirang/Lumla		Garnetiferous micaschist, phyllite, sericite quartzite and tremolite-actinolite marble
---------------------------------------Tectonic/ Unconformity---------------------------------------				
Middle Proterozoic	Bomdila	Intrusives		Granite
		Dailing		Biotite granite gneiss
		Dedza	Upper (Niumi)	Carbonate (Limestone and dolomite) with alteration of greenish, purple and dark grey carbonaceous phyllite
			Lower (Kabak)	Oligomictic conglomerate, quartzite with impersistant bands of dolomite and phyllite
		Tenga	Upper (Reyang)	Basic meta-volcanics and chlorite biotite garnet schist interbedded with flaggy quartzite
			Lower (Garubuthan)	White to grayish white schist, quartzite, purple quartzite with purple silky shale
		Khetabari		Sericite-quartz phyllite, garnetiferous phyllite and schist, graphite/carbonaceous phyllite, quartzite
---Main central thrust (MCT)---				
Lower Proterozoic	Sela	Galensiniak		High grade schist gneiss and migmatites (intruded by younger tourmaline granite and pegmatite of tertiary age)
		Tahila		Graphite schist, calc-silicate, marble, amphibolites and schistose quartzite
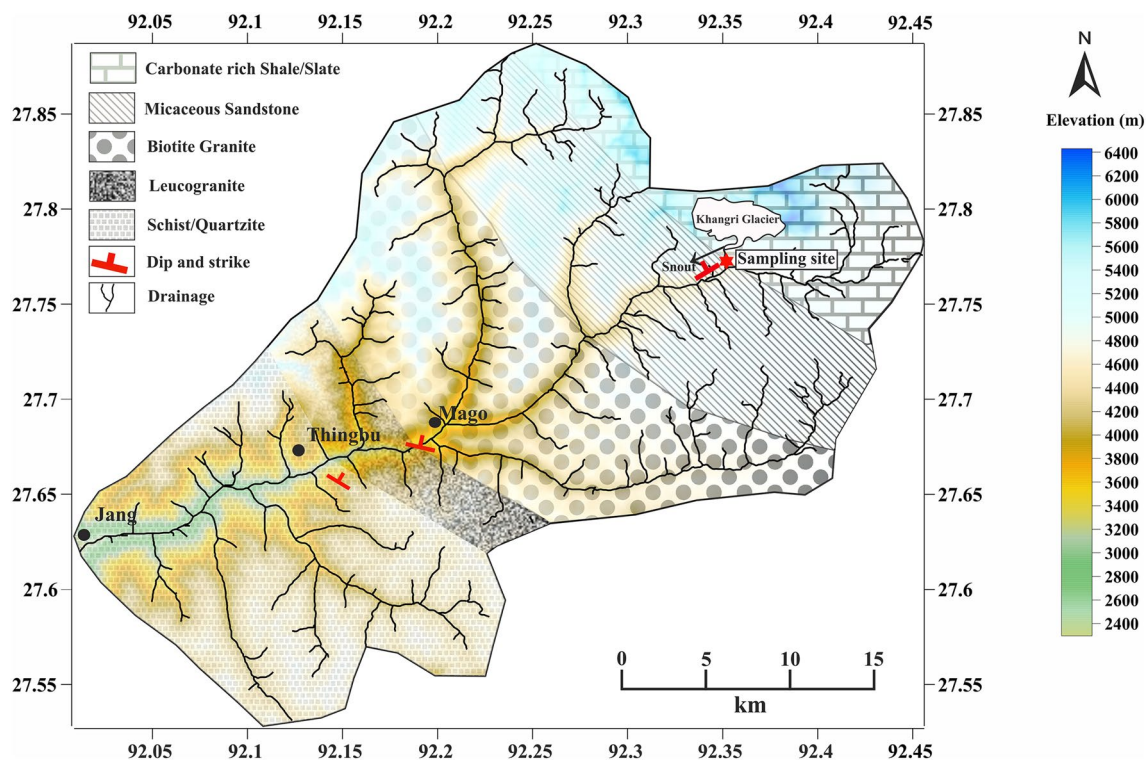
Fig. 3 Simplified geological map of the study area (modified after Bhattacharjee and Nandy 2017)

glacier snout in clear sky conditions, in the month of June to minimize the effect of rainfall and snowfall. The meltwater samples were collected twice continuously for 11 days, in the morning (8:00 AM) and evening (5:00 PM) in 500 ml prewashed plastic bottles for laboratory analysis (Fig. 2e). The collection of water samples was done according to the method suggested by (Ostrem 1975). These sample bottles were tightly closed and placed in a dark environment to avoid changes resulting from the exposure to light. For detailed hydro-chemical analysis, all meltwater samples were carried to the laboratory of G. B. Pant National Institute of Himalayan Environment and Sustainable Development Kosi-Katarml Almora. Along with the water samples fresh rock samples, three of each rock type were collected from 5 km downstream of the snout to ~ 4 km upstream of the snout. These rock samples were collected to know the mineral assemblage of the rocks which contributes ions into the glacial meltwater.

On-site measurement

On-site analysis of electrical conductivity (EC), potential of hydrogen (pH), and total dissolved solids (TDS) of meltwater was carried out according to the standard protocols and methods of American Public Health Association (APHA) (Apha 1995) using different calibrated standard instruments. The pH, EC, and TDS of the meltwater samples were measured using an EC and pH probe (New Professional Tri meter). The EC probe was calibrated using a standard solution (1430 μs/cm) and pH probe was calibrated using two standard buffer solution (pH 4.0 and 7.0), before taking the measurements. The meltwater sample was filtered using a Whatman filter paper no. 42, and the filtrate water was measured by the portable instrument (PCS tester 35) to determine the TDS.

Discharge measurement

Channel discharge has been calculated using area–velocity methods (Eq. 1), in which velocity and cross-sectional area of the channel (Fig. 4) through which water flows have been calculated by the standard surveying technique as described by (Hubbard and Glassar 2005). In this technique, transects across the stream are measured at 20 cm interval which is expressed as the depth of the channel bed form the water surface. The flow velocity of the channel was measured using timing floats (wooden floats) over the surface of the stream. The flow velocity decreases exponentially towards the channel bed as well as towards the bank from its centre for which a correction factor $k = 0.8$ (Hubbard and Glassar 2005) has been used to calculate the mean channel velocity. The meltwater discharge (Q) is calculated using the following formula (Hubbard and Glassar 2005).
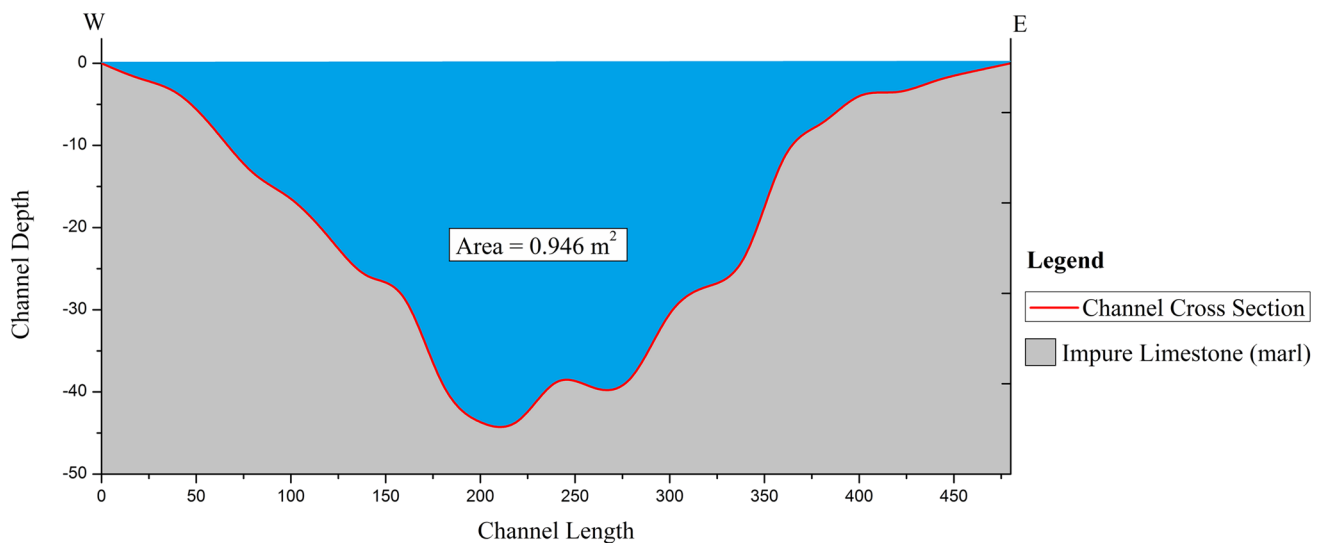
$$Q = k\,(A \times V), \tag{1}$$

Fig. 4 Cross section across the stream draining from the snout of Khangri Glacier

where Q is meltwater discharge, k is correction factor (0.8) for calculating mean channel velocity, A is cross-sectional area of the channel, and V is the surface velocity of the channel.

Laboratory analysis

Hydrochemical analysis

The measurement of Total Suspended Sediment (TSS) was carried out by the vacuum filtration process. In this process, a fixed volume of water sample was poured from a pre-weighed 0.45 μm Millipore membrane filters. After the completion of filtering process, the filter paper was dried in an oven at 100 °C for 3–4 h. The filter paper was then weighed, and the gain in filter paper weight represented the TSS, expressed in terms of mass per volume of sample filtered. The chemical analysis of meltwater samples was done using a standard method (APHA 2005). Na^+ and K^+ were determined through the help of Flame Photometer (Photometer 128). The concentration of Ca^{+2} and Mg^{+2} was determined by EDTA titration method as well as HCO_3^- and Cl^- were measured by acid titration method. The concentration of NO_3^- and SO_4^{2-} was analyzed using a spectrophotometer (Eppendorf AG 22331) and photometer (Paqualb photometer 5000), respectively. The Rock Ware, Inc. Aq.QA software version 1.5 was used for plotting Piper diagram and identification of hydro-chemical facies. The Statistical Package for Social Science (SPSS) version 10.5 was used for correlation matrix between different physicochemical parameters.

Petrographic analysis

The rocks present near the snout of the glacier are metasedimentary shales and slates (Fig. 2f), while the granitoid rocks are exposed ~ 6 km downstream from the present position of snout. The thin section of these rocks was made of thickness 30 microns and the rocks were observed under transmitted light under a petrological microscope. A detailed petrography was done and the approximate mineral assemblage was calculated through point counting technique by taking 500 points for each thin section using Gazzi–Dickinson method (Gazzi 1966; Dickinson 1970).

Results and discussion

Variation in ionic concentration of meltwater

The hydro-chemical analysis of meltwater draining from Khangri glacier has been carried out to assess the major ion chemistry and contribution of weathering process in dissolve ions. The onsite and laboratory analyses of physical and chemical characteristics of glacier meltwater with maximum, minimum, and average values of analytes are shown in Table 2. The close examination of this table shows that there is no major difference in the chemical parameters of the morning and the evening water samples; however, physical parameters (EC and TDS) of the morning water samples of Khangri Glacier meltwater are higher than the evening samples. This difference in the physical parameters of morning and evening samples was probably because of variation in meltwater discharge. In

Table 2 Physicochemical parameters of Khangri glacier meltwater and their ionic concentration ratios with maximum, minimum, and average values

Sample No.	MNG/ EVE	EC	pH	TDS	TSS	Ca²⁺	Mg²⁺	Na⁺	K⁺	HCO₃⁻	SO₄²⁻
KG1	EVE	105.4	6.81	53.86	0.085	23.87	18.86	3.39	2.07	244	51
KG2	MNG	107.1	6.94	54.74	0.085	22.71	19.76	3.4	2.08	259.25	50
KG3	EVE	101.5	6.77	51.83	0.082	24.23	20.47	3.29	1.96	274.5	49
KG4	MNG	102.7	6.79	52.45	0.082	23.55	19.42	3.31	2.04	289.5	52
KG5	EVE	106.8	6.85	53.59	0.085	22.71	19.35	3.37	2.06	305	46
KG6	MNG	108.8	6.98	54.63	0.086	21.03	19.23	3.46	2.1	259.25	44
KG7	EVE	105.2	6.82	53.75	0.084	22.71	19.37	3.36	2.05	274.5	48
KG8	MNG	107.8	6.94	54.11	0.086	23.55	19.79	3.31	2.04	244	50
KG9	EVE	105.9	6.87	54.12	0.084	20.52	18.84	3.37	2.07	259.25	44
KG10	MNG	107.4	6.92	55.9	0.085	20.28	19.25	3.38	2.08	305	47
KG11	EVE	105.3	6.83	53.81	0.084	23.18	21.4	3.28	2.09	366	46
KG12	MNG	106.8	6.91	54.59	0.085	26.71	20.86	3.32	2.03	320.25	57
KG13	EVE	107.1	6.93	54.74	0.085	25.26	20.35	3.3	2.06	289.75	52
KG14	MNG	107.4	6.94	54.9	0.086	24.39	20.2	3.41	2.09	289.75	51
KG15	EVE	105.4	6.89	53.86	0.085	17.66	20.89	3.31	2.03	320.25	50
KG16	MNG	106.6	6.86	54.48	0.085	21.87	19.37	3.41	2.07	259.25	54
KG17	EVE	107.8	7.07	55.11	0.086	25.47	21.15	3.42	2.08	335.5	52
KG18	MNG	110.9	6.97	56.72	0.087	24.39	20.33	3.35	2.05	274.5	53
KG19	EVE	103.2	6.71	53.71	0.084	20.18	18.84	3.32	2.05	244	44
KG20	MNG	105.8	6.83	54.07	0.085	27.75	18.4	3.31	2.04	244	43
KG21	EVE	104.6	6.85	53.44	0.084	23.87	18.81	3.34	2.06	228.75	40
KG22	MNG	105.2	6.88	53.75	0.084	21.87	19.28	3.43	2.09	259.25	50
Max.		110.9	7.07	56.72	0.087	27.75	21.39	3.46	2.1	366	57
Min.		101.5	6.71	51.83	0.082	17.66	18.39	3.28	1.96	228.75	40
Avg.		106.1	6.88	54.19	0.085	23.09	19.73	3.35	2.05	279.35	48.72
St. Dev.		2.064	0.08	1.03	0.001	2.618	0.848	0.05	0.03	34.71	4.10

Table 2 (continued)

Sample No.	MNG/EVE	NO_3^-	Cl^-	Na^+/Cl^-	K^+/Cl^-	A	B	C	CR	SR
KG1	EVE	6.13	0.947	3.581	2.187	7.83	0.113	0.89	0.827	0.173
KG2	MNG	6.18	0.355	9.577	5.859	7.75	0.114	0.89	0.838	0.162
KG3	EVE	6.14	0.355	9.268	5.521	8.52	0.105	0.89	0.849	0.151
KG4	MNG	6.15	0.71	4.662	2.873	8.03	0.111	0.89	0.848	0.152
KG5	EVE	6.1	0.473	7.12	4.352	7.75	0.114	0.89	0.869	0.131
KG6	MNG	6.21	0.473	7.31	4.437	7.24	0.121	0.88	0.855	0.145
KG7	EVE	6.09	0.473	7.099	4.331	7.78	0.114	0.89	0.851	0.149
KG8	MNG	6.08	0.71	4.662	2.873	8.1	0.11	0.89	0.83	0.17
KG9	EVE	6.13	0.71	4.746	2.915	7.23	0.121	0.88	0.855	0.145
KG10	MNG	6.17	0.71	4.761	2.93	7.24	0.121	0.88	0.866	0.134
KG11	EVE	6.1	0.947	3.465	2.098	8.30	0.108	0.89	0.888	0.112
KG12	MNG	6.07	0.473	7.014	4.289	8.89	0.101	0.9	0.849	0.151
KG13	EVE	6.15	0.473	6.972	4.352	8.50	0.105	0.89	0.848	0.152
KG14	MNG	6.22	0.71	4.803	2.944	8.10	0.11	0.89	0.85	0.15
KG15	EVE	6.13	0.71	4.662	2.859	7.40	0.119	0.88	0.865	0.135
KG16	MNG	6.21	0.71	4.803	2.915	7.52	0.117	0.88	0.828	0.172
KG17	EVE	6.17	0.568	6.021	3.662	8.48	0.106	0.89	0.866	0.134
KG18	MNG	6.15	0.473	7.077	4.331	8.28	0.108	0.89	0.838	0.162
KG19	EVE	6.14	0.473	7.014	4.331	7.27	0.121	0.88	0.847	0.153
KG20	MNG	6.05	0.473	6.993	4.31	8.63	0.104	0.9	0.85	0.15
KG21	EVE	6.2	0.71	4.704	2.901	7.90	0.112	0.89	0.851	0.149
KG22	MNG	6.23	0.473	7.246	4.415	7.45	0.118	0.88	0.838	0.162
Max.		6.23	0.946	9.577	5.859	8.892	0.121	0.898	0.884	0.173
Min.		6.05	0.355	3.464	2.091	7.235	0.101	0.878	0.826	0.115
Avg.		6.14	0.595	6.070	3.712	7.913	0.112	0.887	0.850	0.149
SD		0.05	0.169	1.684	1.018	0.399	0.005	0.005	0.018	0.018

$A = (Ca^{2+}+Mg^{2+})/(Na^++K^+)$; $B = (Na^++K^+)/TC^+$; $C = (Ca^{2+}+Mg^{2+})/TC^+$; C ratio $(CR) = [HCO_3^-/(HCO_3^-+SO_4^{2-})]$; S ratio $(SR) = [SO_4^{2-}/(SO_4^{2-}+HCO_3^-)]$.

MNG, morning, *EVE* evening, *SD* standard deviation, *Max* maximum, *Min* minimum, *Avg* average

Unit: all parameters are in mg/l except the EC and pH, EC in µS/cm

the evening, the meltwater discharge is higher than the morning because of high and low solar insolations in afternoon and morning, respectively. The increased discharge dilutes the TDS, whereas low discharge increases the concentration of TDS (Singh et al. 2014). Therefore, during less discharge, the meltwater has higher dissolved ion concentration because of longer contact of meltwater with the solute (basal lithology) and high residence time, which is mainly responsible for the higher values of EC and TDS in the morning time. The measured conductivity of meltwater samples ranges from 101.5 to 110.9 μs/cm, with an average value 106.12 μs/cm. The variation in EC depends upon the concentration of TDS in the meltwater. EC is generally considered as a measure of TDS and depends on the ionic potency of solution (Sharma et al. 2013). The TDS values of meltwater vary from 51.82 to 56.72 mg/l with an average of 54.18 ± 1.02 mg/l. The variability in TDS mainly depends on the dilution of solute in glacier meltwater (Rainwater and Guy 1961). The ratio of TDS (mg/l) to EC (μs/cm) is commonly accepted as 0.7 for fresh water (Meybeck 1984). The average TDS/EC ratio was 0.511 ± 0.001 for Khangri glacier meltwater which is in agreement that the water is slightly fresh. The pH results of all the meltwater samples are found to be range in between 6.71 and 7.07, with average value of 6.88 which is almost neutral to slightly acidic. The bedrocks weathering, ablation zone, accumulation zone, and lateral moraines are the major sources of sediments' concentration in glacial fed streams (Singh et al. 2003). The TSS concentration varied in range from 0.0816 to 0.0872 mg/l with an average 0.0847 ± 0.001 mg/l. This shows less fluctuation in the concentration of suspended sediment in the study area, which directly represents the small variation in meltwater discharge (Kumar et al. 2002).

The cationic results from the laboratory analysis show that the average concentration Ca^{+2} varied from 17.66 to 27.75 mg/l with average (23.08 ± 2.61 mg/l) followed by Mg^{+2} 18.39 to 21.39 mg/l (19.73 ± 0.84 mg/l), Na^+ 3.28 to 3.46 mg/l (3.35 ± 0.05 mg/l), and K^+ 1.96 to 2.1 mg/l (2.05 ± 0.03 mg/l). The result shows that calcium is the most abundant cation followed by magnesium, sodium, and potassium which constituting 47.86%, 40.91%, 6.95%, and 4.25% of the total cations, respectively. The anionic concentration varied from 228.75 to 366 mg/l for HCO_3^- with average (279.35 ± 34.70 mg/l) followed by SO_4^{2-} 40–57 mg/l (48.72 ± 4.10 mg/l), NO_3^- 6.05–6.23 mg/l (6.14 ± 0.05 mg/l), and Cl^- 0.35–0.94 mg/l (0.59 ± 0.16 mg/l). HCO_3^- is the most dominant anion followed by SO_4^{2-}, NO_3^-, and Cl^- which constituting 84.86, 14.80, 1.86, and 0.18% of the total anions, respectively.

Ionic flux computation

There are a limited number of studies on glacial solute fluxes, which is often limited by a fundamental lack of discharge observations (Hasnain and Thayyen 1999; Hodson et al. 2000). In this study, daily average meltwater discharge and ion denudation rates of Khangri Glacier meltwater have been calculated during ablation period. The cation denudation rate (R^+) is calculated using the following formula (Fang et al. 2012):

$$F^+ = \sum_{i=1}^{n} C_i^+(t) \times Q(t) \tag{2}$$

$$R^+ = \frac{F^+}{m}, \tag{3}$$

where F^+ is total cation flux, C_i^+ is the cation concentration (Ca^{+2}, Mg^{+2}, Na^+, and K^+) present in the meltwater, Q is the meltwater discharge, t refers to a particular time period, R^+ is the cation denudation rate of the catchment area, and m is area of the catchment. Similarly, the total anion flux F^- and anion denudation rate of the catchment R^- have been calculated.

The meltwater discharge, Ion Flux (IF) of the individual ion species, F^+ (total cation flux), F^- (total anion flux), R^+ (cation denudation rate), and R^- (anion denudation rate) of the catchment area is given in Table 3. The Khangri glacier catchment covers an area of ~9.5 km² and the daily average meltwater discharge is 3.90×10^7 l. The results shows that calcium has the highest (0.90 ton/day), while potassium has the lowest (0.08 ton/day) cationic flux, whereas the bicarbonate contributes towards highest (10.89 ton/day) and chlorine towards lowest (0.02 ton/day) anionic flux. The total ionic flux of the meltwater is 14.94 tons/day, which will be around 2286.37 tons for the ablation period (May–September) (Table 3). The cation and anion denudation rates of the Khangri Glacier catchment are 0.19 and 1.37 ton/km²/day and will be around 30.30 and 210.36 tons for the ablation period. The anion denudation is 74.81% higher than the cation denudation rate.

Weathering processes and sources of solutes in glacier meltwater

The concentration of dissolved ions in glacier meltwater mainly depends on the bed rock mineralogy, rock–water interaction, weathering reactions, composition of atmospheric inputs, and velocity of water flow (Singh and Hasnain 1998). The chemical weathering of rocks beneath the glacier is responsible for the variation in chemical composition of glacier meltwater (Raiswell 1984). The rocks

Table 3 Daily and ablation period's meltwater discharge, Individual Ion Flux (IIF), cation flux (F^+), anion flux (F^-), cation denudation rate (R^+), and anion denudation rate (R^-) of the catchment area

	Analytes								Total
	Ca^{2+}	Mg^{2+}	Na^+	K^+	HCO_3^-	SO_4^{-2}	NO_3^{-2}	Cl^-	
IIF (ton/day)	0.90	0.76	0.13	0.08	10.89	1.90	0.23	0.02	14.94
IIF (ablation period)	137.81	117.80	20.03	12.25	1667.4	290.8	36.67	3.55	2286.37
F^+ (ton/day)	⊢---------- 1.88 ----------⊣								
F^+ (ablation period)	⊢---------- 287.90 ----------⊣								
F^- (ton/day)					⊢---------- 13.06 ----------⊣				
F^- (ablation period)					⊢---------- 1998.47 ----------⊣				
R^+ (ton/km²/day)	⊢---------- 0.19 ----------⊣								
R^+ (ablation period)	⊢---------- 30.30 ----------⊣								
R^- (ton/km²/day)					⊢---------- 1.37 ----------⊣				
R^- (ablation period)					⊢---------- 210.36 ----------⊣				
Discharge	3.9×10^7 liter per day; 5.96×10^9 liters (ablation period)								

Catchment Area (9.5 sq km)

Ablation period (May–September)
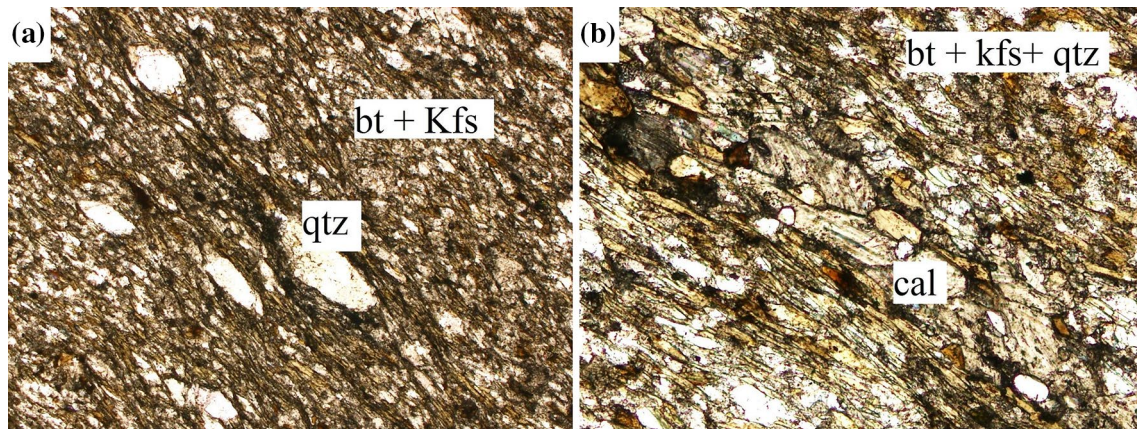
Fig. 5 Microphotographs of the rocks exposed near to the snout of glacier. **a** Foliated shales and slates consisting of quartz porphyroblast in the matrix of biotite. **b** Impure limestone, i.e., marls consisting of calcite porphyroblast in the matrix of biotite and feldspar. *cal* calcite, *qtz* quartz, *kfls* K feldspar, *bt* biotite

exposed near the snout are slightly metamorphosed shales and slates consisting of porphyroblast of quartz (Fig. 5a) and calcite (Fig. 5b) in the matrix mainly composed of biotite and feldspar. These carbonate-rich metasediments have an average composition of biotite (15–17%), feldspar (10–12%), calcite (25–28%), quartz (37–42%), and ~2% others (ilmenite + hematite + apatite) (Fig. 5b). The dissolution of calcite from these metasedimentary rocks is one of the primary sources of calcium into the water. Ca^{+2} and Mg^{+2} are the most dominated cations in the glacial meltwater which shows a good relation with the minerals abundance present in the rocks. Calcite ($CaCO_3$) and biotite $K(Mg,Fe)_3AlSi_3O_{10}(F,OH)_2$ are the most abundant minerals in the rocks near to the snout of glacier with K feldspar ($KAlSi_3O_8$) and quartz (SiO_2). This suggests that Ca^{+2} has definitely entered into the water due to the dissolution of calcite and Ca feldspar, while biotite is one of the major sources of Mg^{+2} in glacier meltwater. In meltwater, Na^+

has been derived from chemical weathering of sodium feldspars, i.e., albite ($NaAlSi_3O_8$), and K^+ is derived from K feldspar ($KAlSi_3O_8$) and biotite $K(Mg,Fe)_3AlSi_3O_{10}(F,OH)_2$. The studies of solute provenance are important to assess the balance between silicate and carbonate weathering driven by atmospherically derived CO_2 (White et al. 1999). The sources of chemical composition in reservoir from dissolution of silicates and carbonates are explained by cationic exuberance and their ratios (Singh et al. 2005. The scatter plot between $(Ca+Mg)$ and SO_4^{2-} (Fig. 6) shows strong linear correlation ($r^2 = 0.89$) and all the points fall above the 1:1 equiline indicates $MgSO_4$- and $CaSO_4$-rich rocks supply sulphate in the meltwater. The scatter plot between $(Ca+Mg)$ and TC^+ (Fig. 7) shows that all points fall above 1:1 equiline with an average ratio of (0.88 ± 0.004). The high contribution of $(Ca+Mg)$ to the total cations (TC^+) and high elemental ratio of $(Ca+Mg)/(Na+K)$ (7.91 ± 0.39 mg/l) suggest that carbonate weathering is a major source of dissolved ions in Khangri glacier meltwater. The scatter plot between $(Na+K)$ and TC^+ (Fig. 8) shows that all points lie below 1:1 equiline with low elemental ratio of $(Na+K)/TC^+$ (0.11 ± 0.004) indicates that the chemical composition of meltwater is moderately controlled by silicate weathering. The water draining from carbonate lithology shows high concentration of Ca^{2+} and Mg^{2+} as well as high ratios of Ca/Na (50), Mg/Na (10), and HCO_3/Na (120) (Negrel et al. 1993). The water draining from silicate lithology shows small ratios Ca/Na (0.35), Mg/Na (0.24), and HCO_3/Na (2) (Gaillardet et al. 1999). In the present study, the observed ratios of Ca/Na (6.88 ± 0.82), Mg/Na, (5.88 ± 0.29) and HCO_3/Na (83.28 ± 10.76) are in favor that the ionic concentration of meltwater is mainly influenced by carbonate weathering followed by silicate weathering. HCO_3^- in the natural waters comes from dissolution of carbonate rocks and the disassociation of atmospheric CO_2 (Sharma et al. 2013). The bicarbonate is produced by dissolved CO_2
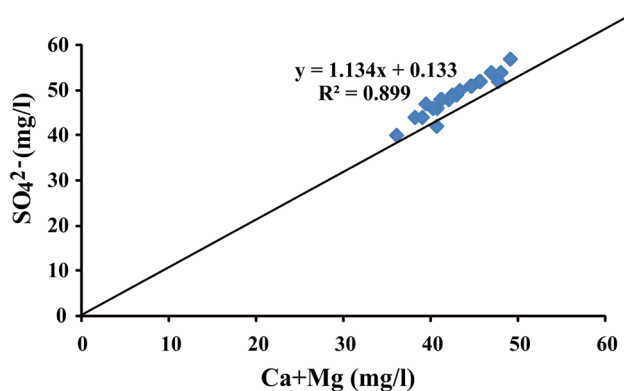

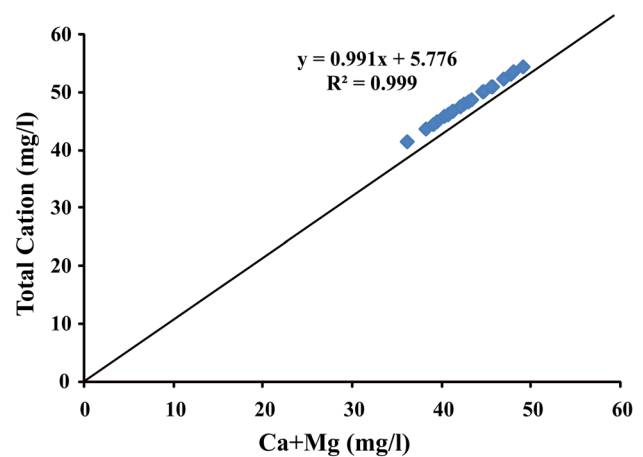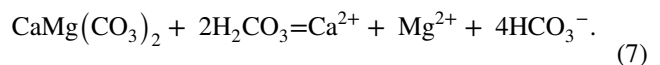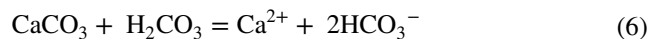**Fig. 7** Scatter plot between $(Ca+Mg)$ and total cations from Khangri glacier meltwater for determining the weathering process in the study area

equations (4) and (5) and dissolution of carbonate equations (6) and (7) as follows:

$$H_2O + CO_2 = H_2CO_3 \tag{4}$$

$$H_2CO_3 = H^+ + HCO_3^-. \tag{5}$$

The carbonic acid (H_2CO_3) reacts with carbonate to produce bicarbonate:

$$CaCO_3 + H_2CO_3 = Ca^{2+} + 2HCO_3^- \tag{6}$$

$$CaMg(CO_3)_2 + 2H_2CO_3 = Ca^{2+} + Mg^{2+} + 4HCO_3^-. \tag{7}$$

These are the important reactions which is responsible for the chemical weathering of rock minerals. The major proton producing mechanism, i.e., sulphide oxidation and
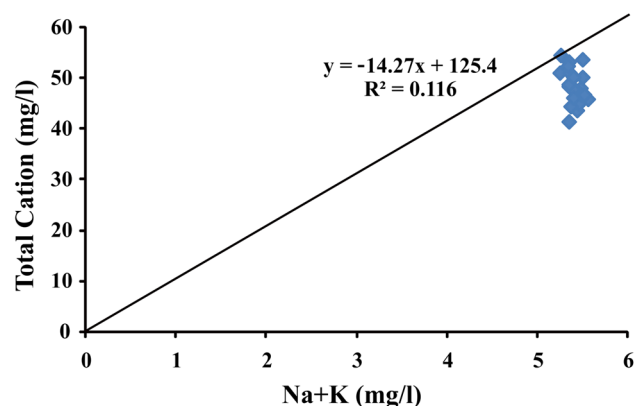

Fig. 6 Scatter plot between $(Ca+Mg)$ and SO_4^{2-} from Khangri glacier meltwater

Fig. 8 Scatter plot between $(Na+K)$ and Total Cations from Khangri glacier meltwater for determining the weathering processes in the study area

carbonation can be evaluated on the basis of concentration ratio (C ratio) $[HCO_3^-/(HCO_3^-+SO_4^{2-})]$. The C ratio of value close to 1 indicates the weathering by carbonation reaction, whereas the ratio close to 0.5 would reveal that coupled reaction carbonation and sulphide oxidation are involved in the weathering (Brown et al. 1996). In the present study, the average C ratio $[HCO_3^-/(HCO_3^-+SO_4^{2-})]$ of meltwater is 0.85 ± 0.01, which is an evidence of weathering is mainly controlled by carbonation reactions. This also suggests that the protons are mainly derived from the dissociation and dissolution of atmospheric CO_2. The C ratio of Mg^{2+}/Ca^{2+} and $Mg^{2+}/(Mg^{2+}+Ca^{2+})$, if > 0.5, the carbonic acid weathering is dominated in that region (Brown et al. 1996). The C ratio Mg^{2+}/Ca^{2+} (0.86) and $Mg^{2+}/(Mg^{2+}+Ca^{2+})$ (0.52) is greater than the 0.5 in the present study which indicates dominance of carbonic acid weathering that can cause dissolution of biotite, which is the one of the most abundant mineral present in the rocks near to the snout of the glacier. In addition, the S ratio $[SO_4^{2-}/(SO_4^{2-}+HCO_3^-)]$ near 0.5 indicates coupled reaction by sulphide oxidation and carbonate dissolution, while the ratio near 0 shows carbonation reaction (Tranter et al. 1997). The average value of S ratio (0.1 ± 0.01) derived from the current study also confirmed the weathering in study area by carbonation reaction. The ocean water contains high concentration of Cl^- in comparison with most of the rocks, so the atmospheric inputs are assessed by the elemental ratio between Cl^- and other elements (Kumar et al. 2008). The elemental ratio $(Na + K)/Cl$ (9.78 ± 2.70) in Khangri glacier meltwater shows higher values, indicating a lower input from marine aerosols. The average equivalent ratio of Na^+/Cl^- (6.07 ± 1.68) and K^+/Cl^- (3.71 ± 1.01) is considerably higher than those of marine aerosols $(Na^+/Cl^- = 0.85$ and $K^+/Cl^- = 0.0176)$ also indicating low contribution from atmospheric inputs in glacier meltwater.

Trilinear classification and effective CO_2 pressure

A Piper diagram also referred as Trilinear diagram (Piper 1944) is a suitable method to classify and compare of hydrochemical facies or water type based on the ionic composition of water samples (Hem 1985). The Piper plot (Fig. 9) shows that majority of samples falls into the earth alkaline metal $(Ca + Mg)$, which is much higher than the alkali $(Na + K)$. Furthermore, the percentage value of weak acid $(HCO_3 + CO_3)$ is higher than the strong acid $(SO_4 + Cl)$. The overall results derived from the Piper diagram show that $Mg–HCO_3$ is the most dominated hydro-chemical facies

Fig. 9 Piper plot for major ionic concentration of meltwater to determine their hydro-chemical facies
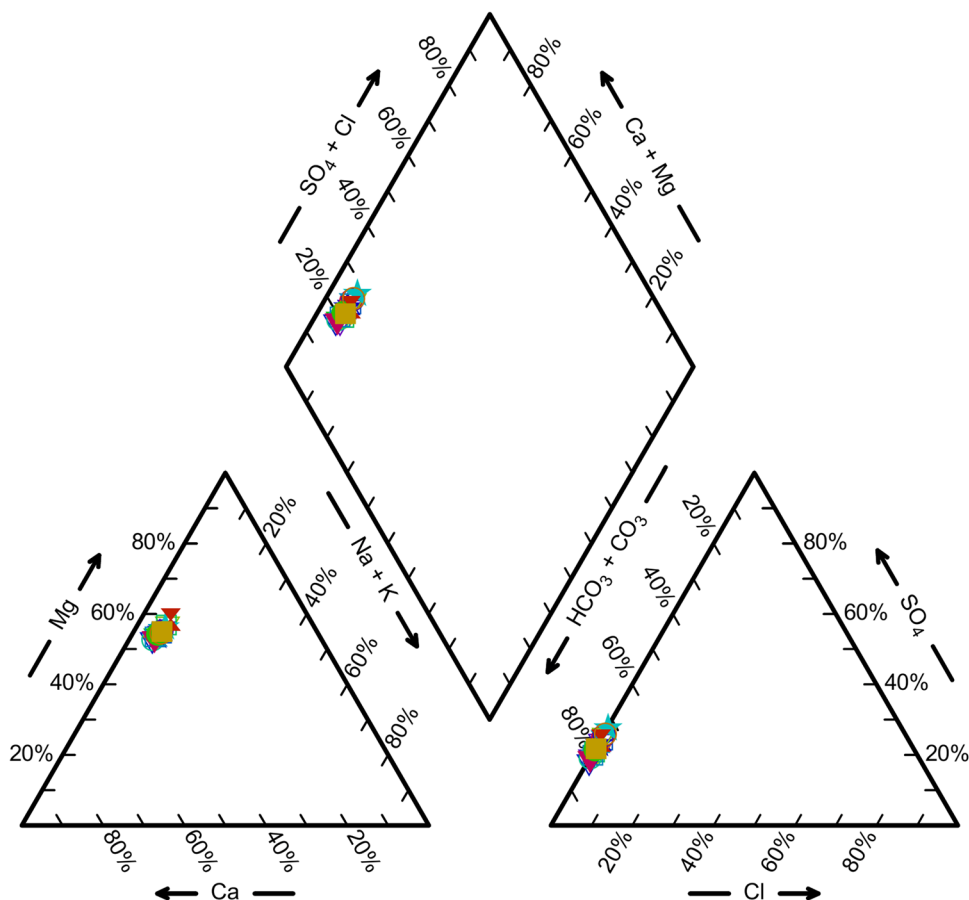
followed by Ca–HCO$_3$-type water. The hydro-chemical facies of meltwater suggested that the water chemistry has evolved through the dissolution of carbonate minerals, e.g., Dolomite [CaMg (CO$_3$)$_2$] and Calcite (CaCO$_3$). The partial CO$_2$ pressure (pCO$_2$) in Khangri glacier was analyzed from HCO$_3^-$ concentration and pH values using the Aq.QA 1.5 software. pCO$_2$ of a solution reflects the rate of CO$_2$ diffusion comparative to the rate of other weathering reaction (Thomas and Raiswell 1984). The high and low pCO$_2$ conditions of CO$_2$ in solution are produced when the supply of protons is higher than their usage and when the requirement of protons for chemical weathering is more than the rate of CO$_2$ diffusion, respectively (Wadham et al. 1998). In general, it is observed that the stream water always shows disequilibrium with the atmosphere (Raymahasay 1986). In extreme cold conditions (glaciated regions), CO$_2$ has a higher rate of solubility in comparison with the release in the atmosphere (Stumm and Morgan 1981). The results obtained from the present study suggests higher solubility of CO$_2$ in meltwater with an average pCO$_2$ value ($10^{-1.5}$ atm) which is higher than the atmospheric value ($10^{-3.5}$ atm), pointing towards an open system weathering and in disequilibrium state with atmosphere.

Statistical analysis

Correlation matrix is a bivariate method generally used to measure the relationship between two variable and degree of dependency of one variable to other variable. A correlation can only provide a presence or an absence of a relationship, not the nature of relationship. On scatter plot diagrams, the correlation coefficient 'r' measures the direction and strength of a linear relationship between two variables. The value of 'r' always lies between -1 and $+1$, where -1 and $+1$ value shows a perfect negative and perfect positive

linear relationship, respectively. The values between (-0.7 and -1) and (0.7 and 1) show a strong negative and positive linear relationship, respectively (Rumsey 2016). The positive values of 'r' indicate positive correlation between two variables (i.e., change in two variables take place in the same direction), whereas negative values of 'r' indicate negative correlation (i.e., change in both variables take place in opposite direction) (Kothari 2004). A multi-parametric correlation matrix between measured parameters of Khangri glacier meltwater samples is represented in Table 4. The correlation matrix shows that the EC has a strong positive correlation with TDS ($r^2 = 0.93$) and TSS ($r^2 = 0.94$). It indicates that EC is directly related to ions dissolved in the meltwater and suspended sediment concentration from surrounding rock and soil. Ca^{2+} is showing strong correlation ($r^2 = 0.94$) with Mg^{2+} and K$^+$ is showing strong correlation ($r^2 = 0.83$) with Na$^+$, indicating similar provenance of their origin. HCO$_3^-$ is showing strong positive correlation ($r^2 = 0.85$) with Mg^{2+} followed by Ca^{2+} ($r^2 = 0.78$) which suggests that these ions are highly compatible with each other and the presence and the absence of Ca^{+2} or Mg^{+2} in the provenance can significantly control the amount of bicarbonate in the water.

Conclusion

The Khangri glacier meltwater is of Mg–HCO$_3$-type hydrochemical facies, and the pH of the meltwater is almost neutral to slightly acidic (6.88). The cation abundance of glacial meltwater in decreasing order is Ca^{+2}, Mg^{+2}, Na$^+$, and K$^+$, whereas the anion abundance is HCO$_3^-$, SO$_4^{2-}$, NO$_3^-$, and Cl$^-$. The meltwater discharge from the Khangri glacier is 5.96×10^9 l for the ablation period, which carries a total ion flux of 2286.37 tons of which the total anions (F$^-$, 13.06 tons/day) contribute 74% more than total cations

Table 4 Correlation matrix between different physical and chemical parameters measured from the Khangri glacier meltwater

	TSS	TDS	EC	pH	Ca	Mg	K	Na	HCO$_3$	Cl	SO$_4$	NO$_3$
TSS	1											
TDS	**0.913**	1										
EC	**0.943**	**0.937**	1									
pH	0.775	0.779	**0.823**	1								
Ca	-0.02	0.148	0.063	0.301	1							
Mg	0.083	0.271	0.174	0.409	**0.949**	1						
K	0.618	0.466	0.517	0.484	-0.44	-0.43	1					
Na	0.492	0.371	0.443	0.483	-0.29	-0.26	**0.831**	1				
HCO$_3$	0.007	0.229	0.114	0.284	**0.779**	**0.854**	-0.389	-0.23	1			
Cl	-0.06	-0.03	-0.06	-0.1	0.092	0.034	-0.039	-0.08	0.145	1		
SO$_4$	0.456	0.222	0.138	0.343	0.934	0.956	-0.393	-0.21	**0.84**	0.107	1	
NO$_3$	0.154	0.119	0.127	0.298	-0.08	-0.08	0.569	0.674	-0.19	-0.02	0.2	1

The bold values indicating strong correlation among different measured parameters

Pearson correlation between different physical and chemical parameters

(F^+; 1.88 ton/day, 287.90 tons for ablation period). Among major cations, the calcium ion contributes the highest (0.90 tons per day and 137.81 tons for ablation period) values of the total cation flux (F^+), while potassium contributes the least (0.08 tons per day and 12.25 tons during the ablation period). Among anions, bicarbonate contributes the highest (10.69 tons per day, 1667.39 during ablation period), whereas chlorine contributes the least (0.02 tons per day and 3.55 tons during ablation period) of the total anion flux (F^-). The anion denudation rates (1.37 tons/Km^2/day, 210.36 tons/Km^2 for ablation period) are seven times higher than the cation denudation rates (0.19 tons/Km^{-2}/day, 30.30 tons/Km^2 for ablation period). The cation denudation rates of Khangri glacier are much higher despite its large catchment area mainly because of its high discharge and presence of carbonate-rich metasedimentary shale and slates which are very susceptible to chemical weathering. The elemental ratio of $(Ca+Mg)/(Na+K)$ is found to be higher and a lower ratio of $(Na+K)/(total\ cations)$ is observed, which elucidates that the chemical composition of meltwater is mainly controlled by carbonate weathering and moderately by silicate weathering. The scatter plot between $(Ca+Mg)$ and total cations also favors towards carbonate weathering. The C ratio $[HCO_3/(HCO_3+SO_4)]$ and S ratio $[SO_4^{2-}/(SO_4^{2-}+HCO_3^-)]$ also point towards, weathering through carbonation reaction. The petrological studies confirm that carbonate-rich metasediments are present near the snout of the glacier. These rocks are rich in calcite and biotite which contributes ions such as Ca^{+2}, Mg^{+2}, and Na^+ and K^+, reflected in the hydrochemistry of meltwater. A relatively high elemental ratio of Na^+/Cl^- and K^+/Cl^- than those of marine aerosols revealed that there is a low contribution of ions from atmosphere. The meltwater of Kangari glacier has a higher pCO_2 value than those of atmospheric values, which suggests that the glacial meltwater has a higher solubility of CO_2 in comparison with its release into the atmosphere, such that the dissolved CO_2 in the meltwater remains in disequilibrium with the atmosphere. The study agrees that the glacial environments are natural laboratories for studying chemical weathering processes in its pristine natural form and the contribution of mineral and rocks towards water chemistry. Khangri glacier is one of the ideal places to study the natural control on chemical weathering because of very less anthropogenic and atmospheric interferences, and there is a need of other studies related to hydrology, precipitation chemistry, and geochemistry in different parts of Arunachal Himalayan glaciers.

References

APHA (American Public Health Association) (1995) Standards methods for the examination of water and wastewater, APHA, AWWA, WEF/1995. APHA Publication, Washington, DC

APHA (American Public Health Association) (2005) Standard methods for examination of water and wastewater, 21st edn. American Public Health Association, Washington, DC

Bakliwal PC, Das AK (1971) Geology of parts of Kameng district, NEFA. Unpub. Prog. Rep. GSI for FS-1970-71

Bhadra A, Mishra P, Rajkumari S, Kumar A, Tripathy S (2016) Temporal variation in dry and wet snow cover for Nuranang Catchment of Arunachal Pradesh India. In: 7th International conference on water resources and environment (ICWRER) Kyoto Japan June 5–9, pp 1–6

Bhattacharjee S, Nandy S (2007) Geology of Western Arunachal Himalaya in Parts of Tawang and West Kameng Districts, Arunachal Pradesh. J Geol Soc India 72:199–207

Bhattacharjee S, Nandy S (2017) Petrology and geochemistry of the Himalayan granites from Western Arunachal Pradesh, India. Indian J Geosci 71(2):439–448

Bhusan SK, Bindal CM, Aggarwal RK (1991) Geology of Bomdila Group in Arunachal Pradesh. J Himal Geol 2(2):207–214

Bora L, Kar A, Baruah I, Kalita MC (2006) Hot springs of Tawang and West Kameng districts of Arunachal Pradesh. Curr Sci 91(8):1011–1013

Brown GH, Fuge R (1998a) Trace element chemistry of glacial meltwaters in an Alpine headwater catchment, Headwater control IV: hydrology, water resources and ecology in headwaters, Meran/Merano, Italy, 20–23 April 1998. Int Assoc Hydrol Sci Publ 248:435–442

Brown GH, Tranter M, Sharp M (1996) Subglacial chemical erosion-seasonal variations in solute provenance, Haut glacier d'Arolla, Switzerland. Ann Glaciol 22:25–31

Clow DW, Mast MA (2010) Mechanisms for chemostatic behavior in catchments: implications for CO2 consumption by mineral weathering. Chem Geol 269:40–51

Collins DN (1979a) Hydrochemistry of meltwater draining from an Alpine glacier. Arc Alp Res 11:307–324

Dickinson WR (1970) Interpreting detrital modes of greywake and arkose. J Sediment Pet 40:695–707

Fang F, Zhongqin L, Shuang J, Jhiwen D, Feiteng W (2012) Hydrochemical Characteristics and Solute Dynamics of Meltwater Runoff of Urumqi Glacier No.1, Eastern Tianshan, Northwest China. J Mt Sci 9:472–482

Gaillardet J, Dupre B, Louvat P, Allegre CJ (1999) Global silicate weathering and silicate weathering and CO_2 consumption rates deduced from the chemistry of large rivers. Chem Geol 159:3–30

Gazzi P (1966) Le Arenarie del Flysch Sopracretaceo dell'Appennino Modenese: correlazioni con il Flysch di Monghidoro. Mineralogica e Petrographica Acta 12:69–97

Godsey SE, Kirchner JW, Clow DW (2009) Concentration-discharge relationships reflect chemostatic characteristics of US catchments. Hydrol Proc 23:1844–1864

Hasnain SI, Thayyen RJ (1999) Controls on the major-ion chemistry of the Dokriani glacier meltwaters, Ganga basin, Garhwal Himalaya, India. J Glaciol 45:87–92

Hem JD (1985) Study and interpretation of the chemical characteristics of natural water. 3rd ed. In: U.S. Geol Survey, Water-Supply Paper 2254:65–100

Hodson A, Tranter M, Vaten G (2000) Contemporary rates of chemical denudation and atmospheric CO2 sequestration in glacier basin: an Arctic perspective. Earth Surf Proc Land 25:1447–1471

Hubbard B, Glassar N (2005) Field techniques in glaciology and glacial geomorphology. Wiley, England

Jain LS, Basu RS (1978) Geological mapping of crystallines and other rocks of Higher Himalaya and preliminary investigation for the base metal in the area. Unpub. Prog. Rep. GSI for FS-1976-77

Kesari GK (2010) Geology and Mineral Resources of Arunachal Pradesh. Geol. Survey of India, Miscellaneous Publication, No. 30 (4), Vol 1(i) Arunachal Pradesh

Kothari CR (2004) Research methodology methods and techniques (second revised edition). New Age International (P) Limited, Publishers, New Delhi

Kumar G (2013) Geology of Arunachal Pradesh. Geol Society of India, Banglore

Kumar K, Miral MS, Joshi P, Panda YS (2002) Discharge and suspended sediment in the meltwater of Gangotri glacier, Garhwal Himalaya, India. Hydrol Sci J 47(4):611–619

Kumar K, Miral MS, Joshi S, Pant N, Joshi V, Joshi LM (2008) Solute dynamics of meltwater of Gangotri glacier, Garhwal Himalaya, India. Environ Geology 58:1151–1159

Meybeck M (1984) Atmospheric inputs and river transport of dissolve substances. In: Webb BW (ed) Dissolved loads of rivers and surface water quantity/quality relationships, vol 141. IAHS Publication, Wallingford, pp 173–192

Negrel P, Allegre CJ, Dupre B, Lewin E (1993) Erosion sources determined by inversion of major and trace element ratios in river water: The Congo basin case. Earth Planet Sci Lett 120:59–76

Oliva P, Viers J, Dupré B (2003) Chemical weathering in granitic environments. Chem Geology 202:225–256

Ostrem G (1975) Sediment transport in glacial meltwater stream. In: Jopling AV, McDonald BC (eds) Glacio-fluvial and Glacio-lacustrine sedimentation. Soc of econom palaeontol and mineral, vol 23. SEPM Publisher, USA, pp 101–122

Piper AM (1944) A graphical procedure in the geochemical interpretation of water analysis. Trans Am Geophys Union 25:914–923

Raina VK, Srivastava D (2008) Glacier atlas of India. Geol Soc of India, Bangalore

Rainwater FH, Guy HP (1961) Some observations on the hydrochemistry and sedimentation of the Chamberlain Glacier Area Alaska. In: US Geol Sur Professional Paper 414, pp l–14

Raiswell R (1984) Chemical models of solute acquisition in glacial meltwater. J Glaciol 30(104):49–57

Ramanathan AL (2011) Status Report on Chhota Shigri glacier (Himachal Pradesh). Department of Science and Technology, Ministry of Science and Technology, New Delhi. Himalayan glaciology technical report, Number 1:88

Raymahasay BC (1986) Geochemistry of bicarbonate in river water. J of Geol Soc India 27:114–118

Rumsey DJ (2016) Statistics for dummies. Wiley, England

Senzeba KT, Bhadra A, Bandyopadhyay A (2015) Snowmelt runoff modelling in data scarce Nuranang catchment of eastern Himalayan region. Remote Sensing Appl Soc Environ 1:20–35

Sharma P, Ramanathan AL, Pottakkal J (2013) Study of solute sources and evolution of hydrogeochemical processes of the Chota Shigri Glacier meltwaters, Himanchal Himalaya, India. Hydrol Sci J 58(5):1128–1143

Singh S (1998) Geology of Tawang-Woming La and Gashe La area, Tawang district, Arunachal Pradesh. Unpub. Prog. Rep. GSI for FS 1997-98

Singh AK, Hasnain SI (1998) Major ion chemistry and weathering control in a high altitude basin: Alaknanda river, Garhwal Himalaya, India. Hydrol Sci J 43(6):825–843

Singh P, Ramasastri KS, Kumar N, Bhatnagar NK (2003) Suspended sediment transport from the Dokriani Glacier in the Garhwal Himalayas. Nordic Hydrol 34(3):221–244

Singh AK, Mondal GC, Singh PK, Singh S, Singh TB, Tewary BK (2005) Hydrochemistry of reservoirs of Damodar river basin, India: weathering processes and water quality assessment. Environ Geology 48:1014–1028

Singh P, Haritashya UK, Kumar N (2008) Modelling and estimation of different components of stream flow for Gangotri glacier basin Himalayas. Hydrol Sci J 53:309–322

Singh VB, Ramanathan AL, Pottakkal JG, Sharma P, Linda A, Azam MF, Chatterjee C (2012) Chemical characterization of meltwater draining from Gangotri glacier, Garhwal Himalaya, India. J Earth Sys Sci 121(3):625–636

Souchez RA, Lemmens MM (1987) Solutes. In: Gurnell AM, Clark MJ (eds) Glacio-fluvial sediment transfer. Wiley, UK, pp 285–303

Srivastava RK (2013) Geochemistry of Proterozoic Granitoids exposed between Dirang and Tawang, western Arunachal Himalaya, northeastern India: petrogenitic and tectonic significance. Int J Earth Sci 102:2043–2060

Stumm W, Morgan JJ (1981) An introduction emphasizing chemical equilibria in natural waters. In: Stumm W, Morgan JJ (eds) Aquatic chemistry, 2nd edn. Wiley, New York, pp 230–258

Thomas AG, Raiswell R (1984) Solute acquisition in glacial meltwaters, II Glacier d'Argentiere (French Alps): bulk meltwaters with open system characteristics. J Glaciol 30(104):44–48

Tranter M, Sharp M, Brown GH, Willis IC, Hubbard BP, Nielsen MK, Smart CC, Gordon S, Tulley M, Lamb HR (1997) Variability in the chemical composition of in-situ subglacial meltwaters. Hydrol Proc 11:59–77

Tripathi C, Jain LS, Basu RS (1979) A note on the find of sulphide mineralization in Lumla area, Kameng district, Arunachal Pradesh. Indian Miner 33(2):55

Valdiya KS (1998) Dynamic Himalaya. Universities Press, Hyderabad, pp 3–4

Wadham JL, Hodson AJ, Tranter M, Dowdeswell JA (1998) The hydrochemistry of meltwater draining a polythermal-based, high Arctic glacier, south Svalbard. Hydrol Proc 12:1825–1849

White AF, Bullen TD, Vivit DV, Schulz MS, Clow DW (1999) The role of disseminated calcite in the chemical weathering of granitoid rocks. Geochim Cosmochim Acta 63:1939–1953